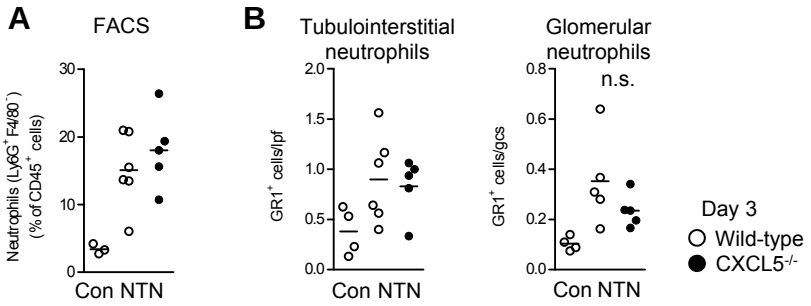

Supplemental Figure 1: Early neutrophil recruitment in WT and CXCL5$^{-/-}$ mice
(**A**) FACS-based quantification of PMN from the kidney of nephritic wild-type, nephritic CXCL5$^{-/-}$ and wild-type control mice at day 3 after induction of nephritis. (**B**) Immunohistochemical quantification of renal PMN infiltration into the tubulointerstitial (per low power field, lpf) and glomerular compartment (per glomerular cross section, gcs) of nephritic WT and CXCL5$^{-/-}$ mice (day 3) using the PMN marker GR1.

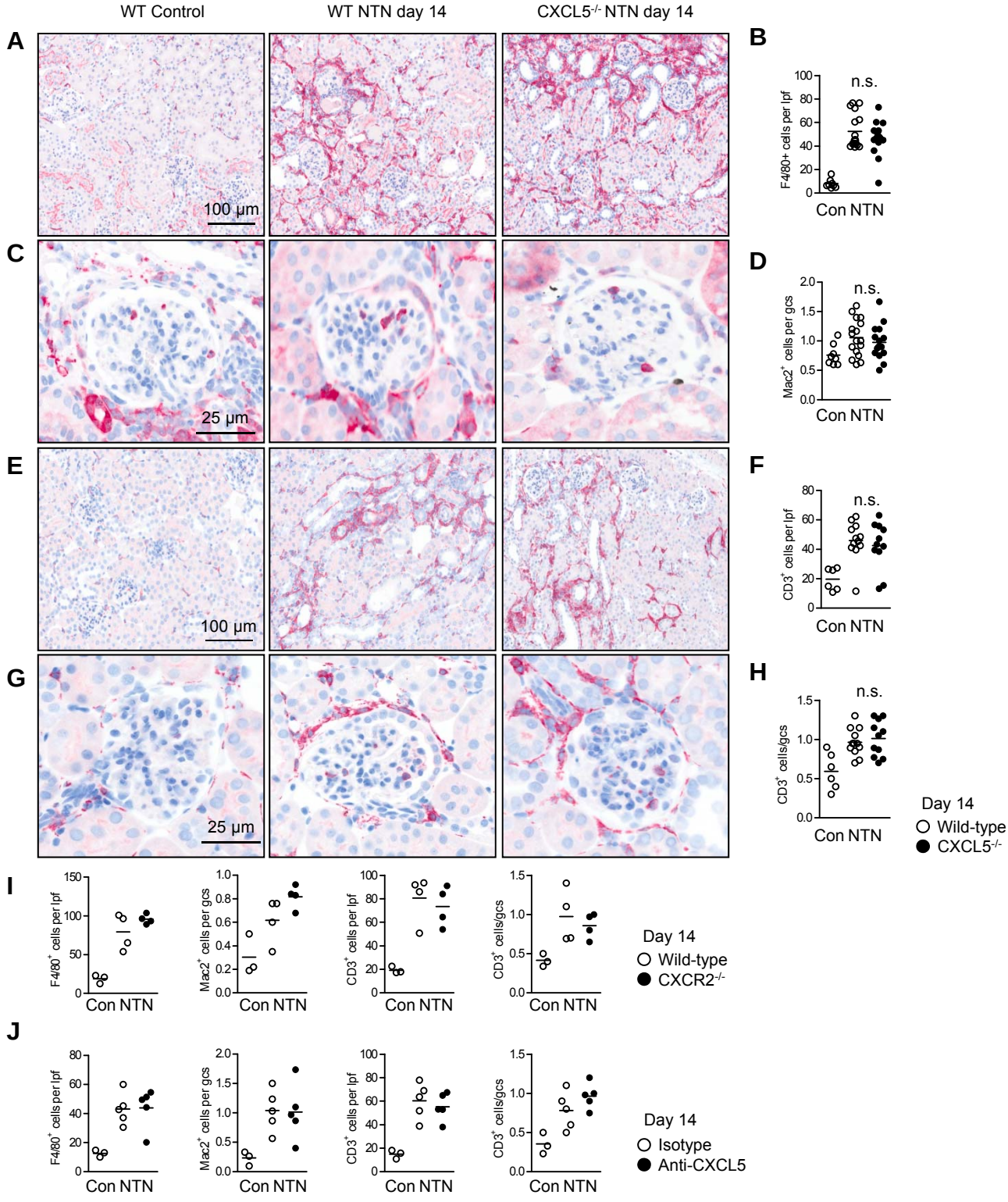

Supplemental Figure 2: Renal leukocyte infiltration

Paraffin-embedded sections (2 µm) were stained with the following antibodies: F4/80 (BM8, BMA, Germany), MAC-2 (M3/38; Cedaralane, Ontario, Canada) and CD3 (A0452, Dako, Germany). Representative immunohistochemical photographs and quantification of renal leukocyte infiltration in nephritic wild-type, nephritic CXCL5$^{-/-}$ and WT control mice at day 14 after induction of nephritis (lpf = low power field; gcs= glomerular cross section) using the macrophage markers F4/80 (**A**, **B**) MAC2 (**C**, **D**) and the T-cell marker CD3 (**E-H**). Original magnification x200 for the tubulointersitial compartment (**A**, **E**) and X400 for the glomerulus (**C, G**). F4/80, MAC-2 and CD3 positive cells were also quantified in CXCR2$^{-/-}$ (**I**) and anti-CXCL5 or IgG2B isotype antibody (**J**) experiments.

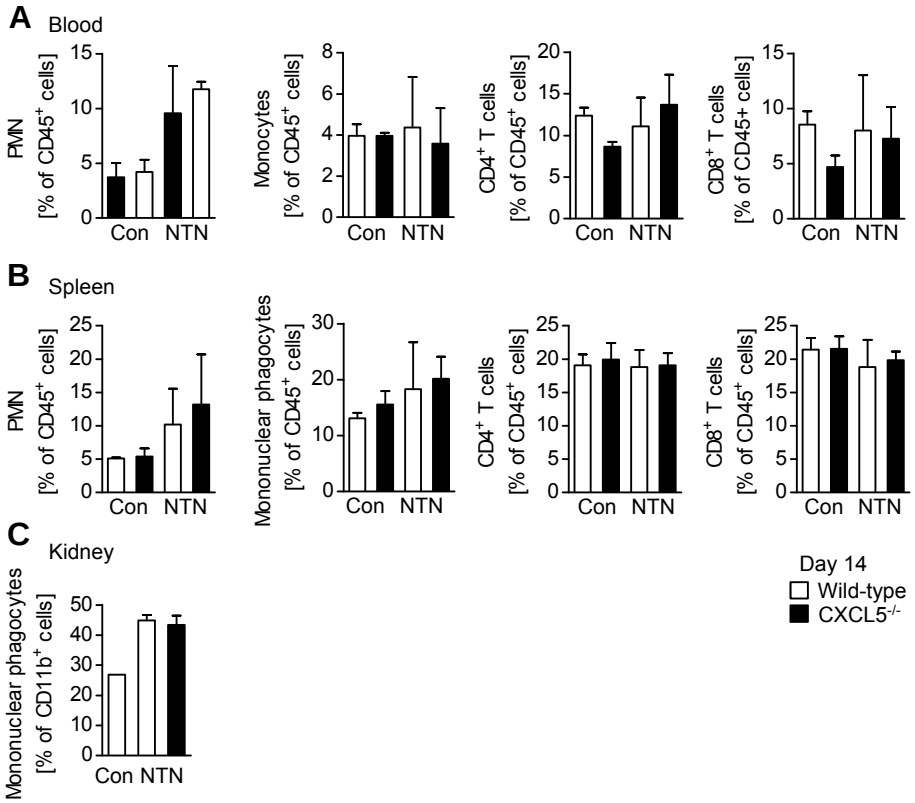

Supplemental Figure 3: Immune cell composition in WT and CXCL5$^{-/-}$ mice

FACS-based quantification of leukocyte subpopulations in the blood (**A**), in the spleen (**B**) and the kidney (**C**) of WT and CXCL5$^{-/-}$ mice at day 14 after induction of NTN. Untreated WT and CXCL5$^{-/-}$ mice served as controls. PMNs were identified as CD45^{+}, CD11b^{+}, Ly6G^{+}, Ly6c^{int} cells. Blood and bone marrow monocytes were identified as CD45^{+}, CD11b^{+}, Ly6G^{-}, Ly6c^{high}. Kidney mononuclear phagocytes were identified as CD45^{+}, CD11b^{+}, Ly6G^{-}, F4/80^{+} cells. CD4^{+} T cells were identified as CD45^{+}, CD3^{+}, CD4^{+} cells and CD8^{+} T cells were identified as CD45^{+}, CD3^{+}, CD8^{+} cells. (n=4-5 per group, bars represent means ± SD).

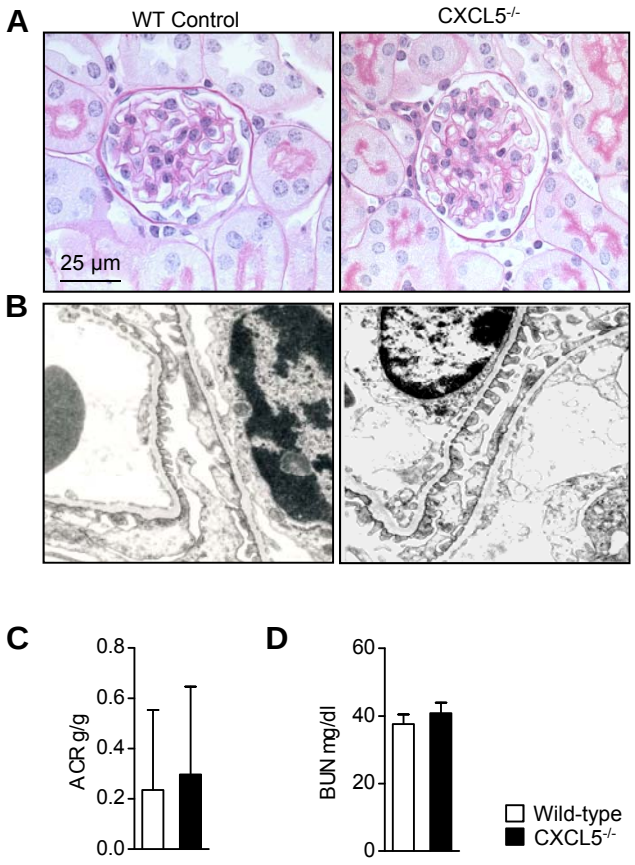

Supplemental Figure 4: Renal phenotype of CXCL5$^{-/-}$ mice

Renal phenotype and function of wild-type and CXCL5$^{-/-}$ mice under homeostatic conditions. (**A**) PAS staining revealed no histologic differences between the knockout and wild-type groups. To analyze possible minimal morphologic abnormalities in the glomerular filtration barrier, we performed electron microscopy. As shown in **B**, no pathologic findings were detectable in both groups in terms of glomerular basement membrane morphology, endothelial cell structure, and podocyte foot process morphology. (**C**+**D**) Functional analysis of CXCL5-deficient and wild-type mice demonstrated identical urinary albumin / creatinine ratio (ACR) and blood urea nitrogen (BUN) levels. (n=4 per group, bars represent means ± SD).

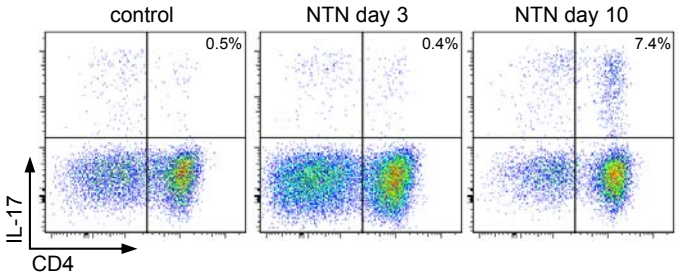

Supplemental Figure 5: Flow cytometry of renal T_H17 cells
Flow cytometric analyses of renal $CD3^+$ T cells isolated from controls and nephritic kidneys at days 3 and 10. Cells were re-stimulated with PMA/ionomycin and intracellularly stained for IL-17A. IL-17-expression by $CD4^+$ T cells peaked at day 10 and was hardly detectable in controls and at day 3. In contrast $CD4^-CD3^+IL\text{-}17^+$ cells (such as γδ T cells, see Turner and Krebs et al. JASN, 23: 1486-1495, 2012) were present in control and nephritic mice at day 3. FACS-plots are representative of each point of time as indicated.

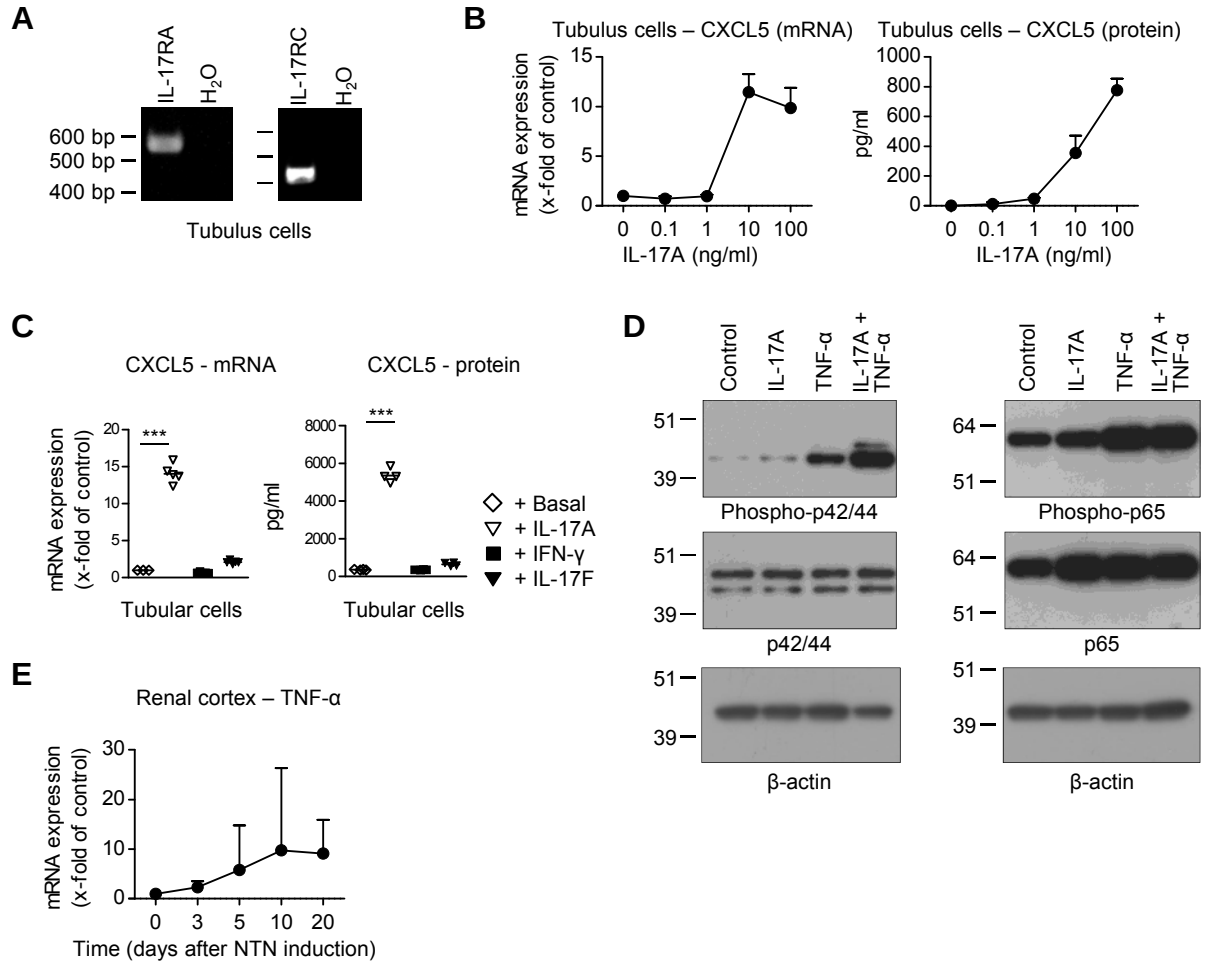

Supplemental Figure 6: IL-17A induces CXCL5 expression in kidney tubular cells
(**A**) Murine epithelial tubular cells express IL-17 receptors IL-17RA and IL-17RC as measured by PCR from cultured cells. (**B**) IL-17A induces dose-dependent CXCL5 expression in cultured tubular cells. (**C**) IL-17A but not IFN-γ or IL-17F induced CXCL5 in cultured tubular cells as measured by RT-PCR (after 4 hours of stimulation) and ELISA from the supernatant (after 24 hours). (**D**) Lysates of stimulated cells were immunoblotted with monoclonal antibodies to phospho-ERK1/2 (upper left) or total ERK1/2 (lower) as well as phospho-p65 and p65 (NF-κB subunit p65, right panel) and β-actin as loading control. (**E**) Quantitative PCR from renal cortex shows TNF-α expression in the kidney in the course of nephrotoxic nephritis. Bars represent means ±SD (***$P < 0.001$).

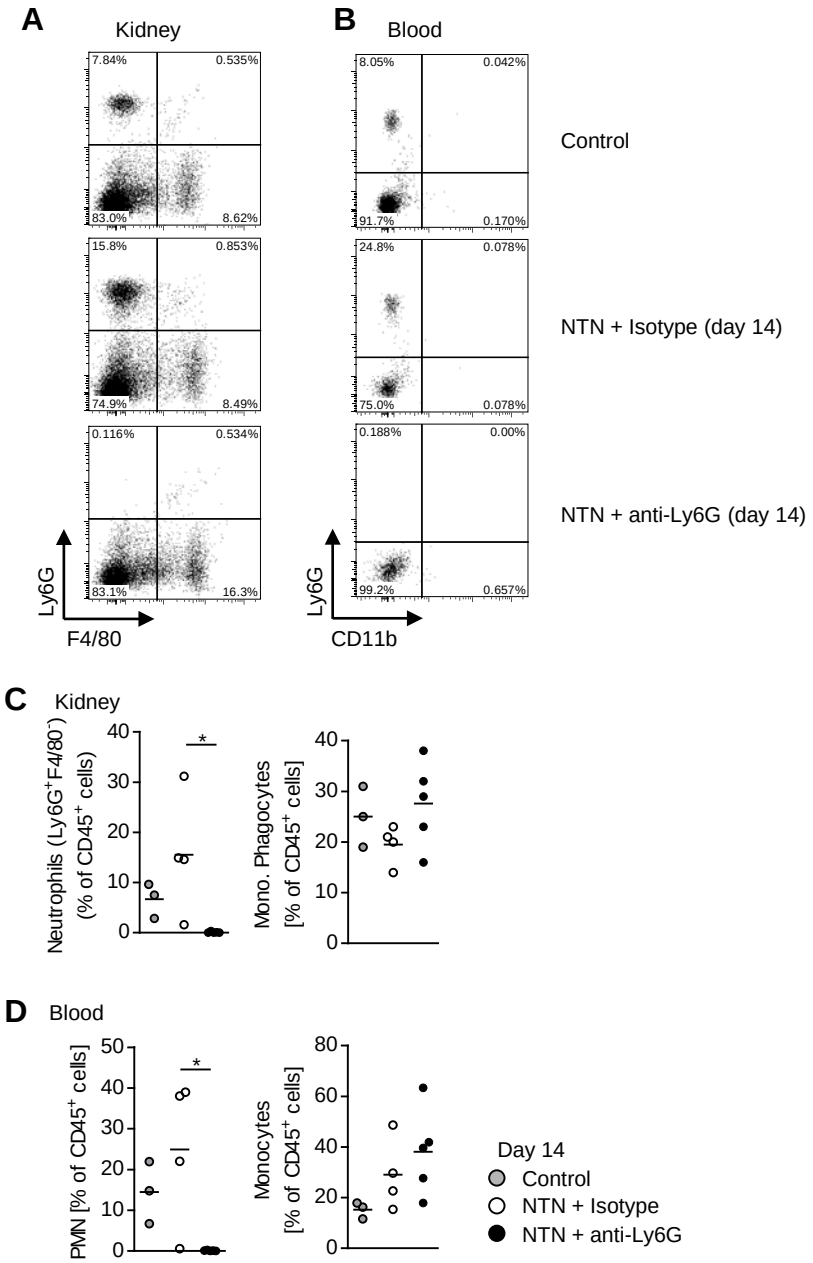

Supplemental Figure 7: Anti-Ly6G-antibody depletes neutrophils *in vivo*

Flow cytometric analysis of leukocytes in the kidney (**A**) and blood (**B**) of nephritic wild-type mice after administration of PMN depleting rat-anti-Ly6G antibody or IgG isotype. Administration of anti-Ly6G was performed every 48 hours for 3 times, starting at day 9 after induction of the disease. Analysis of leukocytes was performed at day 14. Plots are gated on $CD45^+$ and $CD11b^+$ myelo-monocytic leukocytes and were representative for 3 independent experiments. FACS-based quantification of PMN and myelo-monocytic leukocyte subpopulations from the kidney (**C**) and the blood (**D**) of nephritic WT mice after administration of PMN depleting anti-Ly6G antibody or IgG Isotype.

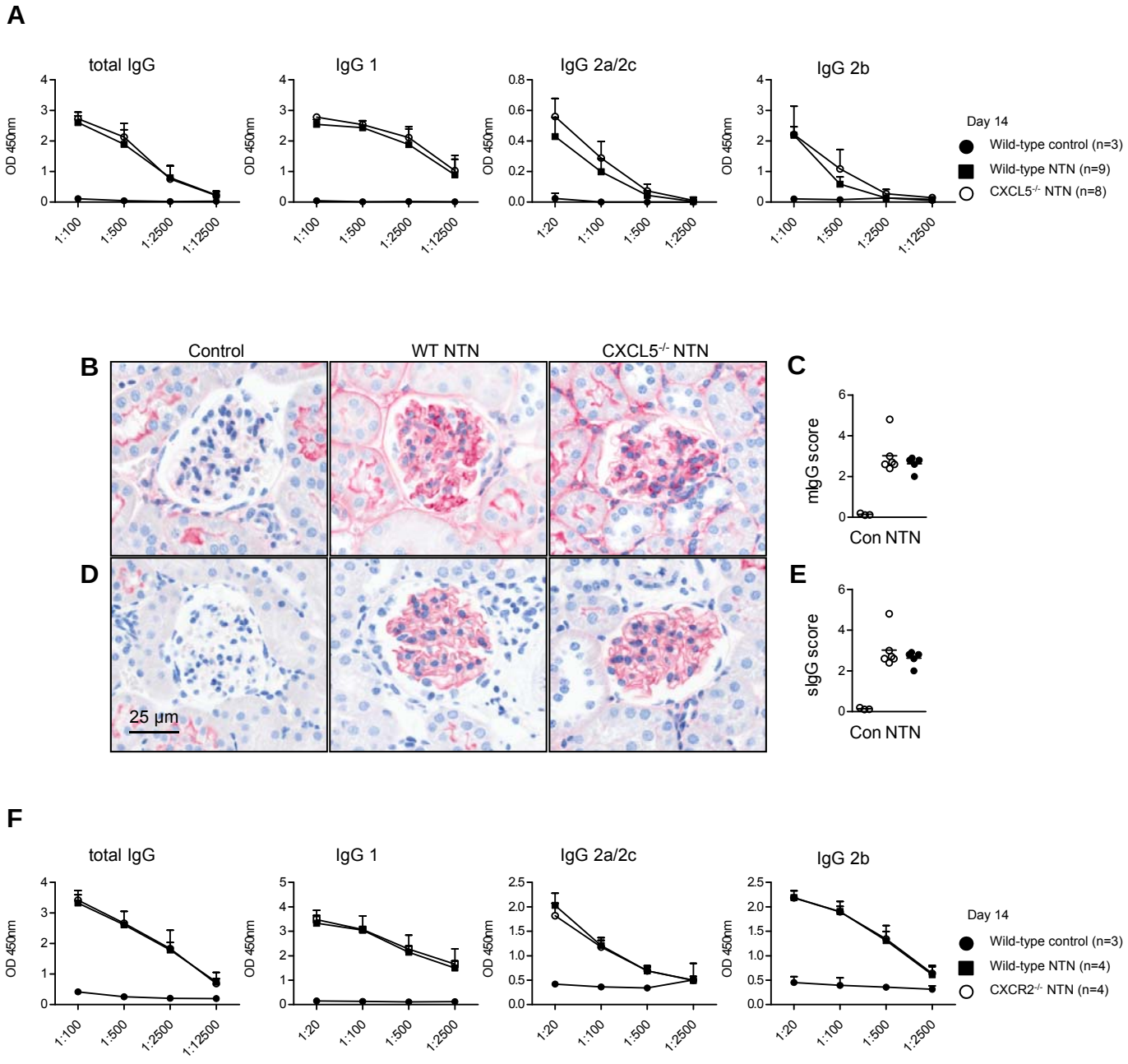

Supplemental Figure 8: Humoral immune response

(**A**) Quantification of mouse anti-sheep specific IgG subclasses present in the serum of nephritic WT or CXCL5$^{-/-}$ mice and non-nephritic WT control mice measured by ELISA. (**B**, **D**) Representative immunohistochemical stainings for glomerular deposition of mouse IgG (**B**) and sheep IgG (**D**) in nephritic wild-type and CXCL5$^{-/-}$ mice 14 days after NTN induction (original magnification x400). (**C**) Quantification of glomerular deposition of mouse IgG (mIgG) and sheep IgG (sIgG) (**E**) in kidney sections of controls, nephritic wild-type, and nephritic CXCL5-deficient mice. (**F**) Quantification of mouse anti-sheep specific IgG subclasses present in the serum of nephritic WT or CXCR2$^{-/-}$ mice and non-nephritic WT control mice measured by ELISA. Bars represent means ± SD (* $P < 0.05$).

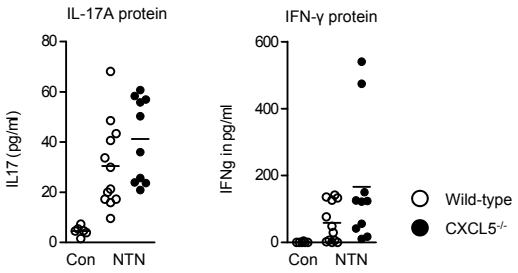

Supplemental Figure 9: Splenocyte supernatants
IL-17A and IFN-γ measurement by ELISA from supernatants of cultured splenocytes from nephritic CXCL5-deficient, nephritic wild-type, and control mice after stimulation with sheep IgG.